CDF Note 10990

Observation of D^0–$\bar{D}^0$ Mixing Using the CDF II Detector

CDF Collaboration

April 18, 2013

Abstract

We measure the time dependence of the ratio of decay rates for the rare decay $D^0 \to K^+\pi^-$ to the Cabibbo-favored decay $D^0 \to K^-\pi^+$. The charge conjugate decays are included. A signal of 33×10^3 $D^{*+} \to \pi^+ D^0$, $D^0 \to K^+\pi^-$ decays is obtained with proper decay times between 0.75 and 10 mean D^0 lifetimes. The data sample was recorded with the CDF II detector at the Fermilab Tevatron and corresponds to an integrated luminosity of 9.6 fb^{-1} for $p\bar{p}$ collisions at $\sqrt{s}$ = 1.96 TeV. Assuming CP conservation, we search for D^0–$\bar{D}^0$ mixing and measure the mixing parameters to be $R_D = (3.51 \pm 0.35) \times 10^{-3}$, $y' = (4.3 \pm 4.3) \times 10^{-3}$, and $x'^2 = (0.08 \pm 0.18) \times 10^{-3}$. We report Bayesian probability contours in the $x'^2 - y'$ plane and find that the no-mixing hypothesis is excluded with a probability equivalent to 6.1 Gaussian standard deviations, providing an observation of D^0–$\bar{D}^0$ mixing from a single experiment.

A neutral meson can spontaneously change into its anti-particle when it is produced in a quantum-mechanical mixed state. The process is referred to as "mixing" and is well established for K^0, B^0, and B_s^0 mesons [1]. The mixing of these mesons is reasonably well-understood within the framework of the standard model with Cabibbo-Kobayashi-Maskawa (CKM) quark-mixing matrix elements that provide a consistent description of many particle decay measurements. Substantial evidence exists for D^0–$\bar{D}^0$ mixing [1, 2, 3, 4, 5], and the process was recently observed in the $K\pi$ channel by the LHCb experiment [6]. In the standard model, D^0–$\bar{D}^0$ mixing is a weak process that occurs primarily through "long-range" virtual intermediate states which consist of common decay channels for particle and anti-particle, such as $\pi^+\pi^-$. The rate for this mixing process has significant theoretical uncertainty as it requires a strong-interaction model and cannot be determined directly from quantum chromodynamics [7]. However, exotic particles could participate in virtual states that lead to mixing, providing indirect evidence for physics beyond the standard model [8]. It is of great interest to establish D^0–$\bar{D}^0$ mixing unambiguously in a specific channel, in a single experiment, and to improve the precision of the measurement of the mixing parameters.

We report a measurement of D^0–$\bar{D}^0$ mixing using the decay $D^0 \to K^+\pi^-$ and its charge-conjugate. In this Letter, reference to a specific decay chain implicitly includes the charge-conjugate decay. The decay $D^0 \to K^+\pi^-$ can arise from mixing of a D^0 state to a $\bar{D}^0$ state, followed by a Cabibbo-favored (CF) decay, or from a doubly-Cabibbo suppressed (DCS) decay of a D^0.

The ratio R of $D^0 \to K^+\pi^-$ to $D^0 \to K^-\pi^+$ decay rates can be approximated [9, 10] as a quadratic function of t/τ, where t is the proper decay time and τ is the mean D^0 lifetime. This form is valid under the assumption of CP conservation and small values for the parameters $x = \Delta m/\Gamma$ and $y = \Delta\Gamma/2\Gamma$, where Δm is the mass difference between the D^0 meson weak eigenstates, $\Delta\Gamma$ is the decay width difference, and Γ is the mean decay width of the eigenstates. Under the assumptions stated above,

$$R(t/\tau) = R_D + \sqrt{R_D}y'\,(t/\tau) + \frac{x'^2 + y'^2}{4}\,(t/\tau)^2, \tag{1}$$

where R_D is the squared modulus of the ratio of DCS to CF amplitudes. The parameters x' and y' are linear combinations of x and y according to the

relations

$$x' = x \cos\delta + y \sin\delta \quad \text{and} \quad y' = -x \sin\delta + y \cos\delta,$$

where δ is the strong interaction phase difference between the DCS and CF amplitudes. In the absence of mixing, $x' = y' = 0$ and $R(t/\tau) = R_D$.

Our measurement uses the full data set collected by the CDF II detector at the Fermilab Tevatron collider, from February 2002 to September 2011, corresponding to an integrated luminosity of 9.6 fb^{-1} for $p\bar{p}$ collisions at $\sqrt{s} = 1.96$ TeV. CDF II [12] is a multi-purpose detector with a magnetic spectrometer surrounded by a calorimeter and a muon detector. The detector components pertinent to this analysis are the silicon microstrip vertex detector, the multi-wire drift chamber (COT), and the 1.4 T magnet which together measure the trajectories and momenta of charged particles. The COT measures ionization energy loss for charged particles, which is used for particle identification (PID). Events are selected in real time with a trigger system developed for a broad class of heavy-flavor decays. The trigger [13] selects events with a pair of oppositely charged particles that are consistent with originating from a decay point separated by at least 200 μm from the beamline, in the transverse plane.

The analysis method used in this measurement is substantially the same as used in a previous measurement [4] based on a subset of the data corresponding to an integrated luminosity of 1.5 fb^{-1}. In the off-line analysis, we reconstruct the "right-sign" (RS) CF decay chain $D^{*+} \to \pi^+ D^0$, $D^0 \to K^-\pi^+$, and the "wrong-sign" (WS) decay chain $D^{*+} \to \pi^+ D^0$, $D^0 \to K^+\pi^-$. The relative charges of the pions determine whether the decay chain is RS (like charge) or WS (opposite charge). The RS and WS D^* decays have the same kinematic distributions, and may differ only in decay time distributions. To reduce systematic uncertainties, we use the same selection criteria (cuts) for both the RS and WS decay modes. Analysis cuts were optimized before the WS candidates were revealed, and were chosen to maximize the expected WS signal significance based on the scaled RS signal and the WS background from sidebands.

The D^0 candidate reconstruction starts with a pair of tracks from oppositely charged particles that satisfy the trigger requirements. The tracks are considered with both $K^-\pi^+$ and π^-K^+ interpretations. A third "tagging"

track, required to have 0.4 GeV/$c \leq p_T \leq$ 2.0 GeV/c , is used to form a D^* candidate when considered as a pion and combined with the D^0 candidate.

We apply two cuts to reduce the background to the WS signal from RS decays where the D^0 decay tracks are misidentified because the kaon and pion assignments are mistakenly interchanged. As determined from the data, 78% of D^0 decays with correct mass assignment are reconstructed with $K\pi$ invariant mass $M_{K\pi}$ within 20 MeV/c^2 of the D^0 mass. The $M_{K\pi}$ distribution for misidentified D^0 decays is much broader, and has only 3.5% of the events within the same mass range. We remove WS candidates that have a RS mass within that range. Thus this cut excludes 96.5% of RS decays and retains 78% of the WS signal. To further reject D^* candidates with misidentified decay tracks, we impose a cut based on PID, described in Ref. [13], which is used to assign D^0 decay tracks as pion or kaon.

We use a series of cuts based on the decay topology of signal events in which a D^* is produced at the collision point, the tagging pion also originates from the collision point, and the D^0 travels a measurable distance before decay. The vertex-based cuts reduce combinatoric background from combinations involving one or more tracks that do not originate from the D^* decay chain of interest. We require the transverse decay length significance to satisfy $L_{xy}/\sigma_{xy} > 4$, where L_{xy} is a measure of the distance between the collision point (measured on an event-by-event basis) and the D^0 decay vertex, in the plane transverse to the beamline. Here $L_{xy} = \vec{r} \cdot \vec{p}_T/p_T$, where $\vec{r}$ is the vector from the collision point to the decay vertex, $\vec{p}_T$ is the transverse component of the momentum of the D^0 candidate with respect to the beamline, and σ_{xy} is the uncertainty on L_{xy}. The transverse impact parameter d_0 is the distance of closest approach in the transverse plane between a track and the collision point. The tagging pion track must have $d_0 < 600$ μm and it must also have a point of closest approach to the collision point less than 1.5 cm along the beamline. To reduce the contribution of D^* mesons produced in beauty particle decays, we require $d_0 < 60$ μm for the D^0 candidate. The remaining contribution of these non-prompt D^* mesons is taken account in the analysis of the time dependence of the WS/RS ratio, as discussed later.

The ratio t/τ is determined for each D^0 candidate by $t/\tau = m_{D^0} L_{xy}/(p_T \tau)$, where $m_{D^0} = 1.8648$ GeV/c^2 and $\tau = 410.1$ fs are the world average values

for the D^0 invariant mass and lifetime, respectively [1]. To study $R(t/\tau)$, we divide the data into 20 bins of t/τ ranging from 0.75 to 10.0, choosing bins of increasing size from 0.25 to 2.0 to reduce statistical uncertainty at larger times. The bin sizes are larger than the t/τ resolution of ≈ 0.16.

After RS and WS candidates are separated into t/τ bins, they are further divided into 60 bins of mass difference $\Delta M \equiv M(K^+\pi^-\pi^+) - M(K^+\pi^-) - M(\pi^+)$ for WS candidates, and analogously for the RS candidates. For each of the 1200 WS and 1200 RS ΔM bins, the D^0 signal yield is determined from the corresponding binned distribution of $M_{K\pi}$. In the fit, the signal shape is modeled by a double-Gaussian with a low-mass tail, and the combinatoric background is modeled by an exponential. For the WS fit, a Gaussian term is included to model the RS background, with shape determined from the data. The signal shape parameters for the WS fits are fixed to the RS values. The D^* signal for each time bin is determined from a least-squares fit of the D^0 signal yield versus ΔM. The signal shape is modeled by a double-Gaussian and an asymmetric tail function. The background shape is modeled by the product of a power law and an exponential. The WS signal shape is fixed to the RS shape. For each $M_{K\pi}$ and ΔM distribution, the parameters for the background shape are allowed to float. The amplitudes of the signal and background are determined independently for all $M_{K\pi}$ and ΔM fits. The RS distributions have similar amounts of background as the WS distributions, but the RS signal is about 230 times larger. A detailed description of the functional forms for the signal and background shapes are described in Ref. [14]. The D^* fit procedure is illustrated for the time-integrated WS ΔM distribution shown in Fig. 1. The fitted WS signal yield is $(3.27 \pm 0.04) \times 10^4$. A fit to the RS ΔM distribution yields a signal of $(7.604 \pm 0.005) \times 10^6$.

The measured ratio R_m of WS to RS signal for each of the 20 t/τ bins is shown in Fig. 2. The data point for each bin is located at the mean value of t/τ for the RS signal in that bin. Each vertical bar shows the uncertainty due to the WS and RS signal estimates. The large uncertainty in the smallest t/τ bin is due to the small event yield caused by the trigger turn-on. After the trigger turn-on, the uncertainties increase with t/τ because of the exponential fall-off in the number of decays.

The expected value of R_m for a given t/τ bin can be expressed in terms

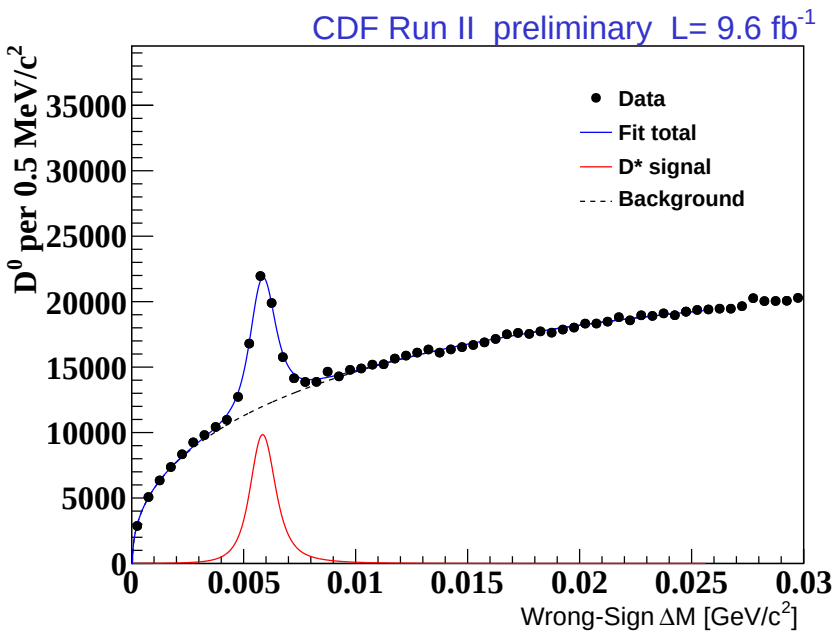

Figure 1: Time-integrated distribution for "wrong-sign" (WS) $D^0 \to K^+\pi^-$ signal yield as a function of ΔM. The signal yield for each bin of ΔM is determined from a fit to the corresponding $M_{K\pi}$ distribution. The result of a least-squares fit to the ΔM distribution is shown.

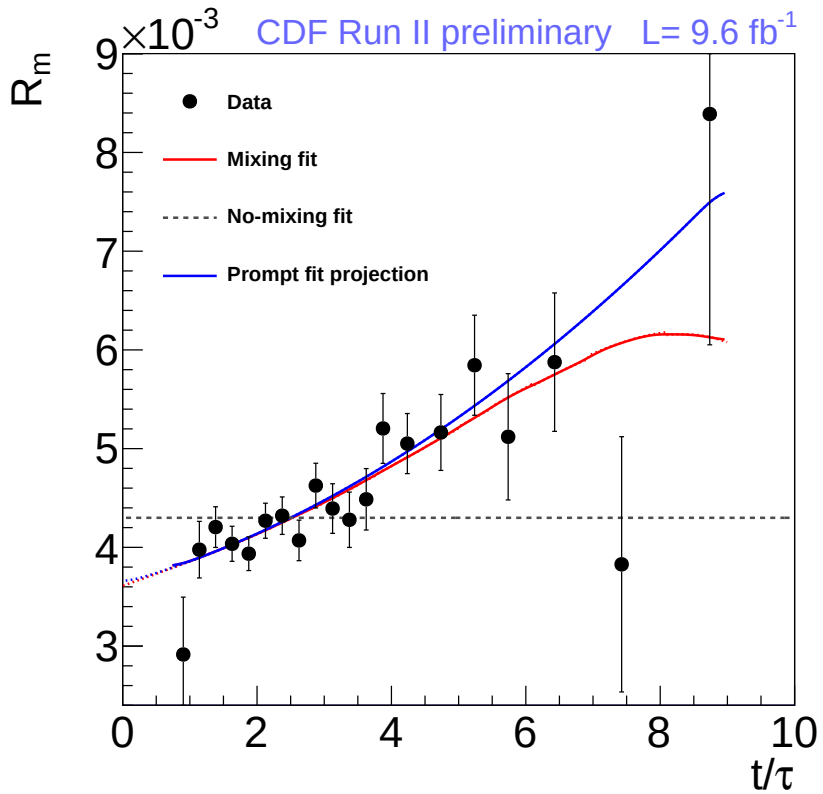

Figure 2: Measured ratio of wrong-sign to right sign D^* decays as a function of normalized proper decay time.

of contributions from prompt and non-prompt production according to,

$$R_m^{pred} = R(t/\tau)\,[1 - f_B(t/\tau)] + R_B(t/\tau) f_B(t/\tau) \tag{2}$$

where $R(t/\tau)$ is the WS/RS ratio of prompt decays given by Eqn. 1, $f_B(t/\tau)$ is the fraction of non-prompt D^* decays and $R_B(t/\tau)$ is the WS/RS ratio of non-prompt D^* decays with measured decay time t. For non-prompt decays, the measured decay time is due to the combination of the decay times for the beauty particle parent and the D^0 daughter. The function $f_B(t/\tau)$ is determined from data and $R_B(t/\tau)$ is determined from a full detector simulation as described below.

The function $f_B(t)$ is determined from the d_0 distribution of RS D^* decays, as illustrated in Fig. 3. For each bin of t/τ, the d_0 distribution is obtained by selecting RS events with $4 < \Delta M < 8$ MeV/c^2 and 1.848 $< M_{K\pi} <$ 1.880 GeV/c^2 ($\pm 2\sigma$) and subtracting the sidebands (low-mass 1.808-1.824 GeV/c^2, high-mass 1.904-1.920 GeV/c^2). The peak at small d_0 is due to the prompt component. The broad distribution extending to large d_0 is due to the non-prompt component. The prompt and non-prompt components are each modeled with the sum of two Gaussians. The fraction f_B is characterized by a 5-parameter polynomial fit in the region $d_0 < 60\mu$m, which is dominated by the prompt component. The value of f_B is (1.5$\pm$0.4)% at $t/\tau = 1.4$ and increases with t/τ due to the faster exponential decay rate for D^0 compared to B. At $t/\tau = 6.4$, the ratio is $(24 \pm 1)\%$.

The function $R_B(t/\tau)$ can be expressed in terms of a function $H(t/\tau, t'/\tau)$ which gives the distribution of non-prompt D^0 decays versus t/τ, as measured from the primary vertex for a given t'/τ, as measured from the B decay vertex. The function h is determined from a full detector simulation of $B \to D^*$ decays for the 20 bins of t/τ, and 100 bins of t'/τ. The function $R_B(t/\tau)$ is given by

$$R_B(t_i/\tau) = \frac{\sum_{j=1}^{100} H(t_i/\tau, t'_j/\tau) R(t'_j/\tau)}{\sum_{j=1}^{100} H(t_i/\tau, t'_j/\tau)}. \tag{3}$$

Note that R_B depends directly on the prompt D^* WS/RS ratio defined in Eqn. 1.

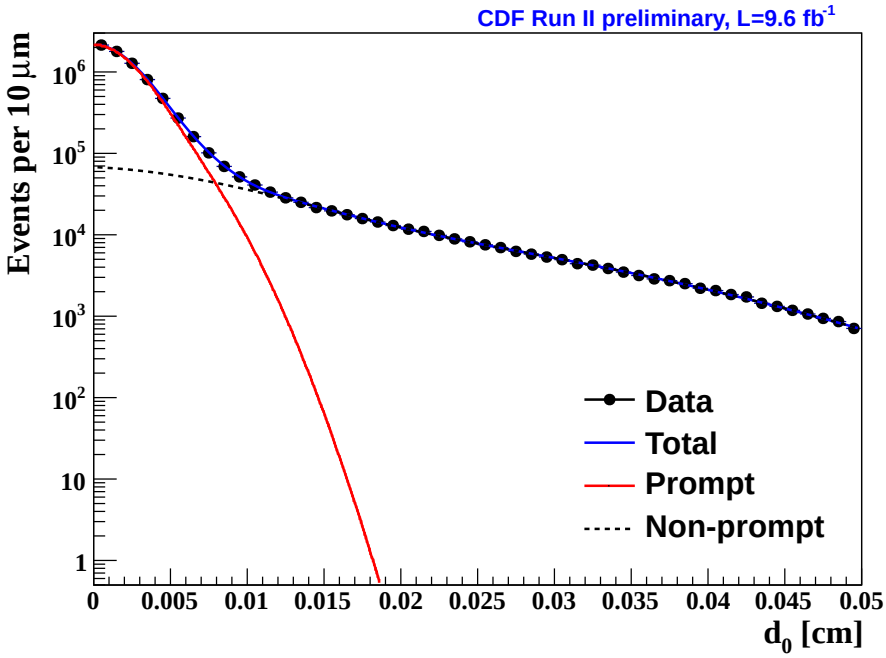

Figure 3: Distribution of transverse impact parameter d_0 for right-sign D^0 candidates for all t/τ bins. The narrow peak is due to promptly produced D^0 mesons and the broad distribution is due to non-prompt D^0 mesons from B decay.

To fit for the mixing parameters, we define

$$\chi^2 = \sum_{i=1}^{20} \left[\frac{R_m(t_i/\tau) - R_m^{pred}(t_i/\tau)}{\sigma_i} \right]^2 + C_B + C_H \tag{4}$$

where σ_i is the uncertainty on $R_m(t_i/\tau)$. The term C_B is a Gaussian constraint on the five fitted parameters describing $R_B(t/\tau)$ and C_H is a Gaussian constraint on the 2000 values of $H(t_i/\tau, t'_j/\tau)$. The statistical uncertainties on the $H(t_i/\tau, t'_j/\tau)$ are due to the number of events in the simulation. The mixing parameters R_D, y', and x'^2, and the Gaussian constrained parameters for R_B and H are found by minimizing the χ^2 defined in Eqn. 4.

To check that the analysis procedure is working properly, we simulated distributions of $M_{K\pi}$ and ΔM for different assumed values of the mixing parameters R_D, y', and x'^2. We generated 400 samples for four different sets of mixing parameters. For each parameter set, the distribution of parameters had mean values equal to the assumed ones within statistical accuracy.

We tested the analysis procedure for systematic uncertainties due to a number of possible origins. The effect on the WS signal yields due to the uncertainty in the signal shapes used to fit the $M_{K\pi}$ and Δ_M distributions are studied by independently varying the shape parameters by $\pm 1\sigma$. For all parameters, the resulting variations on the signal yield are negligible compared to the statistical uncertainty. We checked the sensitivity of the WS and RS signals to the assumed shape of the $M_{K\pi}$ background function by using alternative forms for the generated shape in a simulation of the mass distribution. The alternative forms included explicit shapes for backgrounds due to $D^+ \to K^-\pi^+\pi^+$ decays, determined from data, and partially reconstructed charm particle decays, based on a full detector simulation. In both studies, the simulations returned mixing parameters consistent with those generated. To determine the sensitivity of R_m on R_B, we fit the d_0 distributions with an alternate shape function, leading to an alternate form for R_B with larger values at small t/τ. The resulting change in R_m is negligible, which can be understood from the small non-prompt D^* component at small t/τ. To check the sensitivity of R_m on $H(t/\tau, t'/\tau)$, we scale t/τ and t'/τ by $\pm 10\%$. The resulting changes in R_m are negligible compared to statistical uncertainties.

The 3 mixing, 5 f_B , and 2000 H parameters are determined by minimiz-

ing the χ^2 in Eqn.4. The results for the mixing parameters are given in Table 1 and the resulting function $R_m^{pred}(t/\tau)$ is is shown in Fig. 2. The function $R(t/\tau)$, describing the prompt component, is also shown. The two functions differ at large t/τ due to the effect of non-prompt D^* production. A fit assuming no-mixing is shown and is clearly incompatible with the data. We quantify this incompatibility using both Bayesian and frequentist methods.

Table 1: Mixing parameter results and comparison with previous measurements. All results use $D^0 \to K^+\pi^-$ decays and fits assuming no CP violation. The uncertainties include statistical and systematic components. The significance for excluding the no mixing hypothesis is given in terms of the equivalent number of Gaussian standard deviations. The correlation coefficients for this result are -0.97 for $R_D - y'$, 0.90 for $R_D - x'^2$, and -0.98 for $y' - x'^2$.

Expt.	$R_D(10^{-3})$	$y'\,(10^{-3})$	$x'^2\,(10^{-3})$	σ no mixing
CDF (now)	3.51 ± 0.35	4.3 ± 4.3	0.08 ± 0.18	6.1
Belle [11]	3.64 ± 0.17	$0.6\ ^{+4.0}_{-3.9}$	$0.18\ ^{+0.21}_{-0.23}$	2.0
BABAR[2]	3.03 ± 0.19	9.7 ± 5.4	-0.22 ± 0.37	3.9
CDF [4]	3.04 ± 0.55	8.5 ± 7.6	-0.12 ± 0.35	3.8
LHCb [6]	3.52 ± 0.15	7.2 ± 2.4	-0.09 ± 0.13	9.1

We define a likelihood $\mathcal{L} = \exp(-\chi^2/2)$, where χ^2 is defined in Eqn. 4. The probability is $\mathcal{L}/\mathcal{N}$ where the normalization factor $\mathcal{N}$ is the integral of $\mathcal{L}$ over the mixing parameter space. We compute Bayesian contours containing the region with the highest posterior probability. A flat prior is used for the three mixing parameters, and R_D is treated as a nuisance parameter. The Bayesian contours are shown in Fig. 4. The no-mixing point, $y' = x'^2 = 0$, lies on the contour corresponding to 6.1 Gaussian standard deviations.

A frequentist test statistic $\Delta\chi^2$ is formed from the difference in χ^2 between a fit with $y' = x'^2 = 0$ and a fit with all three mixing parameters floating. For the data, $\Delta\chi^2 = 58.75 - 16.91 = 41.84$. A frequentist p-value is obtained by simulating mass distributions for $y' = x'^2 = 0$ and finding $\Delta\chi^2$ with respect to the nominal values, allowing all 3 mixing parameters to float. In 10^10 samples, 6 are found with $\Delta\chi^2 > 41.8$, giving a p-value corresponding to 6.1 σ.

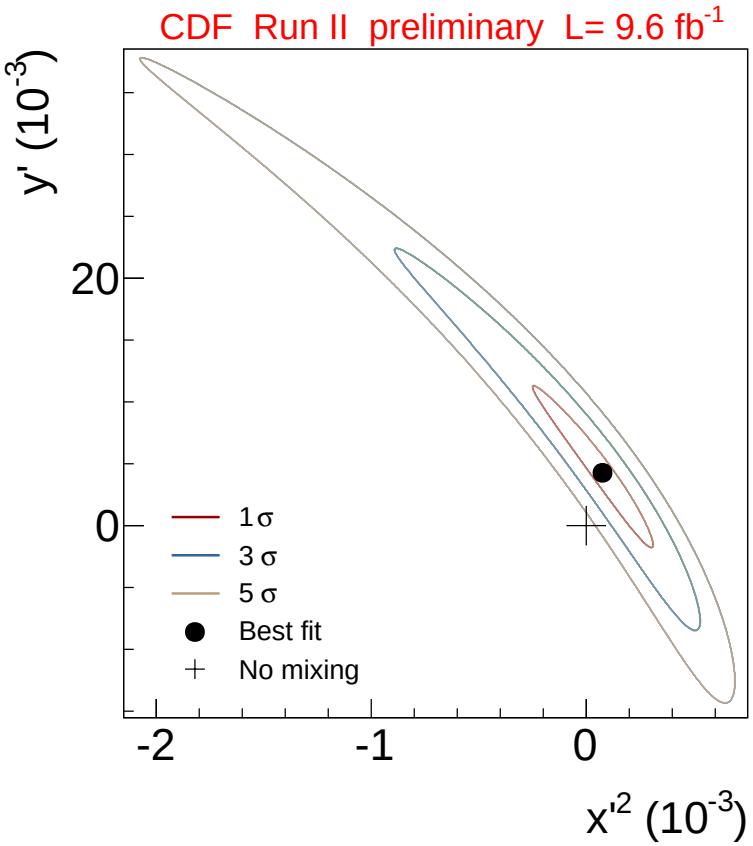

Figure 4: Bayesian probability contours in $x'^2 - y'$ parameter space.

In summary, we measure the time dependence of the ratio of decay rates for the rare decay $D^0 \to K^+\pi^-$ to the Cabibbo-favored decay $D^0 \to K^-\pi^+$. A signal of 33×10^3 $D^{*+} \to \pi^+ D^0$, $D^0 \to K^+\pi^-$ decays is obtained with proper decay times between 0.75 and 10 mean D^0 lifetimes. The data sample was recorded with the CDF II detector at the Fermilab Tevatron and corresponds to an integrated luminosity of 9.6 fb^{-1} for $p\bar{p}$ collisions at $\sqrt{s} = 1.96$ TeV. Assuming CP conservation, we search for D^0–$\bar{D}^0$ mixing and measure the mixing parameters to be $R_D = (3.51 \pm 0.35) \times 10^{-3}$, $y' = (4.3 \pm 4.3) \times 10^{-3}$, and $x'^2 = (0.08 \pm 0.18) \times 10^{-3}$. We report Bayesian probability contours in the $x'^2 - y'$ plane and find that the no-mixing hypothesis is excluded with a probability equivalent to 6.1 Gaussian standard deviations, providing an observation of D^0–$\bar{D}^0$ mixing from a single experiment.

We thank the Fermilab staff and the technical staffs of the participating institutions for their vital contributions. This work was supported by the U.S. Department of Energy and National Science Foundation; the Italian Istituto Nazionale di Fisica Nucleare; the Ministry of Education, Culture, Sports, Science and Technology of Japan; the Natural Sciences and Engineering Research Council of Canada; the National Science Council of the Republic of China; the Swiss National Science Foundation; the A.P. Sloan Foundation; the Bundesministerium für Bildung und Forschung, Germany; the Korean World Class University Program, the National Research Foundation of Korea; the Science and Technology Facilities Council and the Royal Society, UK; the Russian Foundation for Basic Research; the Ministerio de Ciencia e Innovación, and Programa Consolider-Ingenio 2010, Spain; the Slovak R&D Agency; the Academy of Finland; and the Australian Research Council (ARC).

References

[1] J. Beringer *et al.* (Particle Data Group), Phys. Rev. D **86**, 010001 (2012). See especially the review by D. Asner, "D^0–$\bar{D}^0$ Mixing".

[2] B. Aubert *et al.* (*BABAR* Collaboration), Phys. Rev. Lett. **98**, 211802 (2007).

[3] M. Starič *et al.* (Belle Collaboration), Phys. Rev. Lett. **98**, 211803 (2007).

[4] T. Aaltonen *et al.* (CDF Collaboration), Phys. Rev. Lett. **100**, 121802 (2008).

[5] J.P. Lees *et al.* (*BABAR* Collaboration), arXiv:1209.3896 [hep-ex] (2012).

[6] LHCb Collaboration, R. Aaij *et al.* (LHCb Collaboration), Phys. Rev. Lett. **110**, 101802 (2013).

[7] A. F. Falk, Y. Grossman, Z. Ligeti, Y. Nir and A. A. Petrov, Phys. Rev. D **69**, 114021 (2004).

[8] E. Golowich, J. Hewett, S. Pakvasa, and A. A. Petrov, Phys. Rev. D **76**, 095009 (2007).

[9] G. Blaylock, A. Seiden, and Y. Nir, Phys. Lett. B **355**, 555 (1995).

[10] R. Godang *et al.* (CLEO Collaboration), Phys. Rev. Lett. **84**, 5038 (2000).

[11] L. M. Zhang *et al.* (Belle Collaboration), Phys. Rev. Lett. **96**, 151801 (2006).

[12] D. Acosta *et al.* (CDF Collaboration), Phys. Rev. D **71**, 032001 (2005).

[13] A. Abulencia *et al.* (CDF Collaboration), Phys. Rev. D **74**, 031109(R) (2006).

[14] T. Aaltonen *et al.* (CDF Collaboration), Phys. Rev. D **85**, 012009 (2012).